



Effects of internal Acoustic Excitation on the Improvement of Airfoil Performance

Dr. Ikhlas M.Fayed

*Department of Mechanical Engineering
University of Technology*

(Received 3 April 2007; accepted 11 July 2007)

Abstract:

The effect of internal acoustic excitation on the leading-edge, separated boundary layers and the aerodynamic performance of NACA23015 cross section airfoil are examined as a function of excitation location with ranging frequency range (50-400) Hz of the introduced acoustic. Tests are separately conducted in two sections, open type wind tunnels at the Reynolds number of 3.3×10^5 for measurement at angle of attack (0, 3, 6, 9 & 12) deg. and 3×10^4 for the visualization at angle of attack (12) deg. based on the airfoil chord. Results indicated that the excitation frequency and the excitation location are the key parameters to alter the flow properties and thus to improve the aerodynamic performance. The most effective excitation frequency is found to be equal to the shear layer instability frequency and on excitation location close to the separation point. Moreover, the lift is increased and drag reduced dramatically. The corresponding boundary layers are visualized to be reattached to the surface.

Key Words: internal excitation , separation control , NACA

1. Introduction:

There are many circumstances in practice where flow separation plays a major role in determining the flow characteristics. For instance, a wing stall phenomenon may occur when airplane flies at a high angle of attack. It is of great interest to alleviate these problems by applying artificial means so as to suppress and control the flow separation. They founded that sound at particular frequencies and intensities could change the transition process of boundary layer.

The flow field exhibited different characteristic and the momentum exchange is enhanced due to the introduction of the acoustic waves. In accordance with this

observation the control of flow with vertical structures using excitation techniques has been studied extensively in recent years. One of the techniques is called the external acoustic excitation in which the sound is radiated onto the wall from a source outside the flow system.

This technique has been applied by Zaman et al. [1987] which studied the effect of external acoustic excitation about a stall airfoil (LRN-(1)-1007). He founded that a significant improvement in lift was achieved because the tunnel resonance could strongly enhance the outcomes, especially for some cases in which a large amplitude was required.

Yarusevych et al. [2006] studied experimentally the effect of external

acoustic excitation on the wake structure and performance of NACA0025 airfoil. Wind tunnel experiments were carried out for three Reynolds number $(57,100,150) \times 10^3$ and three angle of attack (0,5,10) degree with operating velocity of 2.8 m/s the results establish that external acoustic excitation became effective only when the excitation frequency was close to the tunnel resonance frequency. Furthermore the external excitation required high sound pressure level in order achieves satisfactory results.

To overcome those draw backs an internal excitation technique is used in which the sound is emanated from opening on the wall surface.

This technique has been intensively studied by Hsiao et al. [1990], Chang et al. [1992], and Hsiao et al. [1997] for an airfoil (633-018) performance. Addition study done by Naveh et al. [1998] for an airfoil NACA0015. They indicated that the technique can significantly enhance aerodynamic performance at a relatively modest expense.

The main purpose of this paper is further to examine the effectiveness of the internal acoustically pulsing excitation technique on aerodynamic performance of an airfoil (23015) at angle of attack (0,3,6,9,12). The flow visualization technique will also be carried out to investigate the vertical structure patterns over the airfoil.

2. Experimental facilities:

The investigations were conducted on a suction open-type, subsonic wind tunnel with a 305x305 mm test section (see Fig.1a) . A contraction section with contraction ratio 9:1 and five fine- meshed screens are used for managing the free stream turbulence intensity. Downstream of the working section a diffuser leads to an axial flow fan which is driven by a 506 kW three phase a.c. motor. The flow is controlled by a butterfly valve before exhausting to atmosphere through a

silencer. The tunnel rests on tubular steel supports.

The free stream velocity in the test section was 33.15 m/s. The free stream turbulence intensity of the flow is less than (1.25%) Alan and Harper [1966].

The flow visualization study is carried out in smoke tunnel with working section (100 mm deep) x (180 mm wide) x (240 mm high) fine meshed screens are installed in the settling chamber (see Fig.1b). Smoke line are generated in a wind tunnel by introducing smoke through a small pipe placed in front of a test model, so that the flow around the model is made visible. Photograph systems are used to analyze the flow structure.

Four geometrically NACA23015 airfoil models made of varnished teak wood are employed in this study. The specification of NACA 23015 has been shown in table (1) . Models A&B airfoil of 150mm chord and 305 mm in span was used in subsonic wind tunnel for pressure measurement and models C&D airfoil of 150mm chord and 100mm in span are used for the flow visualization study. As shown in Fig. (1c). For measurement of pressure distribution twenty four pressure taps with 1 mm diameter were installed along the upper (16 taps) and lower surface (8 taps) of airfoil in the mid span of model A&B (see Fig.1d) .

Four narrow slots of 1mm in width and 100 mm in length, located in the mid span are manufactured to omit acoustic wave. The location of slots, from leading edge for models A&C will be at 6.5% chord while models B&D will be at 11.5% chord.

The acoustic generated by loud speaker was funneled into interior of model by 10 mm diameter copper tube. The loud speaker is driven by a power amplifier with a variable frequency function generator. The mean velocity measurement of the test section was made by a Pitot-static tube. The static pressure distribution along the solid body of airfoil is measured by multi-tube manometer to study the aerodynamic

characteristic and the effect of the value when they are excited. The measurement is repeated four times to check the measurement reading then calculated the error measurement (6%).

3. Result and discussions:

Effect of excitation on pressure distributions:

The pressure coefficient normalized by the free stream properties, is defined as

$$Cp = \frac{P - P_\infty}{\frac{1}{2} \rho U_\infty^2} \dots\dots\dots (1)$$

and is used to describe the pressure distributions in the present study.

The surface pressure distributions with and without excitation of the two cases done, one at excitation of 11.5% chord from leading edge at the angles of attack (9 & 12) deg. are presented in Figs.(2&3) respectively while other at excitation of 6% chord for the angle of attack (9 &12) deg. are presented in Fig.(4&5). It clearly reveals that there is significant change in pressure after the sound introduced. However for angle of attack higher than (9) deg. A significant (suction peak) occurs near the leading edge on the upper surface. The larger suction peak area will result in a substantial contribution to the lift for the enhancement of the flow mixing and momentum transport due to internal excitation produces a suction peak at the leading edge of the upper surface airfoil. The suction peaks result in an increase of lift.

When the flow excited at the frequency of (50 Hz) a suction peak is formed, the pressure recovery steadily persists all the way down stream to the trailing edge on the upper surface. Steeper

suction peak is formed when the excitation is increased to 150 as shown in Figs. (3c & 5c) at angle of attack (12)deg.

Effect of Excitation Frequency on Lift:

It has been know that the pressure distribution is sensitive to the disturbance frequency of the acoustic. The lift and drag coefficient have bee defined as :

$$CN = -\int_0^1 (Cp_{uppersurface} - Cp_{lowersurface}) d \frac{x}{c}$$

$$Cc = \int_{y/c}^{y/c} Cp d \frac{y}{c}$$

$$CL = CN \cos \alpha - Cc \sin \alpha$$

$$Cd = CN \sin \alpha + Cc \cos \alpha$$

Figs.(6&7) show the variation of the lift coefficient with angle of attack (3-12)deg. at an excitation frequency ranging from (50 to 400 Hz). Results clearly indicate the sensitivity of the flow. When the angle of attack less than 8 deg., the lift increase is negligible. It then becomes significant as the angle of attack increases.

When the excitation location at 11.5% chord the increase in lift is around 10-20% when the flow is excited within the frequency range from 50 to 150 Hz with peak at frequency 150 Hz at angle of attack (12)deg. as shown in Fig.(6). While for the excitation location 6% was around 15-28.5% for the same angle of attack as shown in Fig.(7).

The contribution from the excitation at other frequency still exists, but it is not so significant. The lift coefficient is improved when the excitation frequency was locked-in to the shear layer, instability frequency of the separated boundary layer and frequency around the natural separation point.

Effect of Excitation Location on Lift:

Two slots located at 6% and 11.5% chord for the acoustic emission are

investigated respectively. Fig. (8) depicts the dependence of the lift on the excitation location at ranging angle of attack (3-12)deg. with frequency 150 Hz. It can be seen that excitation location 6% chord has most significant improvement in lift. In other words the effectiveness of the boundary-layer control with internal excitation strongly depends on the excitation location and excitation at apposition close to separation point is most effective so when the flow is excited near the separation point at the favorable frequency the flow separation is suppressed and maximum lift is increased.

Flow visualization:

The effect of excitation on lift generation is further substantiated by carrying out flow visualization study as depicted in Fig.(9) for the flow with & without excitation at the angle of attack 12 deg. for the location of frequency 6% &11.5% chord. The leading edge separation is clearly revealed when the flow is unexcited Fig. (9a). However when the flow is excited at the shear layer instability frequency of (150 Hz) Figs. (9, b&c) the separated boundary layer in manifested to be reattached to the boundary of the airfoil surface. The reattachment boundary layer will certainly ensure the lift recovery. Also the wake region is narrow due to the boundary reattachment. The excitation location at 6% chord has narrow wake region less than 11.5% chord Fig.(9c), narrow wake with a smaller profile defect indicates a less momentum loss which ensure smaller drag coefficient (higher lift to drag ratio) as seen in Fig. (10) we can conclude that by applying the acoustics internally for the flow excitation at the shear layer instability frequency the double advantages that is higher lift and marrow wake region will assume the higher value of lift to drag ratio.

4. Conclusions:

The study of internal acoustic excitation technique to improve the aerodynamic performance (control flow separation) passing an airfoil is conducted in a suction open type subsonic wind tunnel and a smoke wind tunnel. The technique is quite promising and effective in improving the aerodynamic performance.

The enhancement of the flow mixing and momentum transport due to internal excitation produces a suction peak at the leading edge of the upper surface airfoil. The suction peak results in an increase of lift and narrow wake. Consequently the aerodynamic efficiency (lift-to-drag ratio) is substantially improved when the excitation frequency is locked-in to the shear layer, instability frequency around the natural separation point. The excitation point is most effective and the aerodynamic efficiency is strikingly improved.

Table (1) The specification of NACA 23015.

Upper surface		Lower surface	
X mm	Y mm	X mm	Y mm
0	0	0	0
1.875	5.01	1.875	2.31
3.75	6.66	3.75	3.375
7.5	8.835	7.5	4.56
11.25	10.35	11.25	5.415
15	11.46	15	6.135
22.5	12.78	22.5	7.26

30	13.38	30	8.115
37.5	13.62	37.5	8.67
45	13.575	45	8.94
60	12.885	60	8.88
75	11.61	75	8.25
90	9.915	90	7.215
105	7.875	105	5.865
120	5.595	120	4.245
135	3.06	135	2.385
142.5	1.68	142.5	1.35
150	0	150	0

by *Periodic excitation*”, AIAA Journal, Vol. 35, No.3, 1998.

[7] Alan. P.J. and Harper, “*Low Speed Wind Tunnel Testing* ” John Willey and Sons. Int. 1966.

5. Reference

- [1] K. B. M. Q. Zaman, A Bar-Sever & S. M. Mangalam, "Effect of Acoustic Excitation on the Flow over A low-Re Airfoil" J-Fluid mech, Vol. 182, PP. 127 - 148, 1987.
- [2] Yarusevych S., J. G. Kawall & P.Sullivan , "Influence of Acoustic Excitation on Airfoil Performanc at Low Reynolds Numbers", J.Fluids Engineering, Vol.128, 2006.
- [3] Fei-Bin Hsiao, Chin-Fung Liu, and Jong-Yaw Shyut, "Control of Wall Separated Flow by Internal Acoustic Excitation", Aiaa Journal, Vol. 28, No. 8,1990.
- [4] R. C. Change, F. B. Hsiao, R. N. Shyu, "Forcing Level Effects of Internal Acoustic Excitation on the Improvement of Airfoil Performance", Journal of Aircraft, Vol. 129, No. 5, Sep. - Oct. 1992.
- [5] Hsiao F. B., J. J. Jihand and R. N. Shyn, "The Effect of Acoustics on Flow Passing A High-*AOA* Airfoil", Journal of Sound and Vibration, Vol. 199, No.2, 1997.
- [6] Naveh T, Seifert A, Wagnanski I. "Sweep Effect on Parameters Governing Control of Separation

6. Nomenclature

C	Chord	m
C_c	free coefficient in x direction	---
CL	lift coefficient	---
C_N	free coefficient in x direction	---
C_d	section drag coefficient	---
C_p	pressure coefficient	---
f	frequency	Hz
P	static pressure	N/m²
P_∞	static pressure in free stream	N/m²
U_∞	free stream velocity	m/s
x	Distance along surface airfoil	---
y	Perpendicular distance on airfoil surface	---
ρ	fluid density	kg/m³

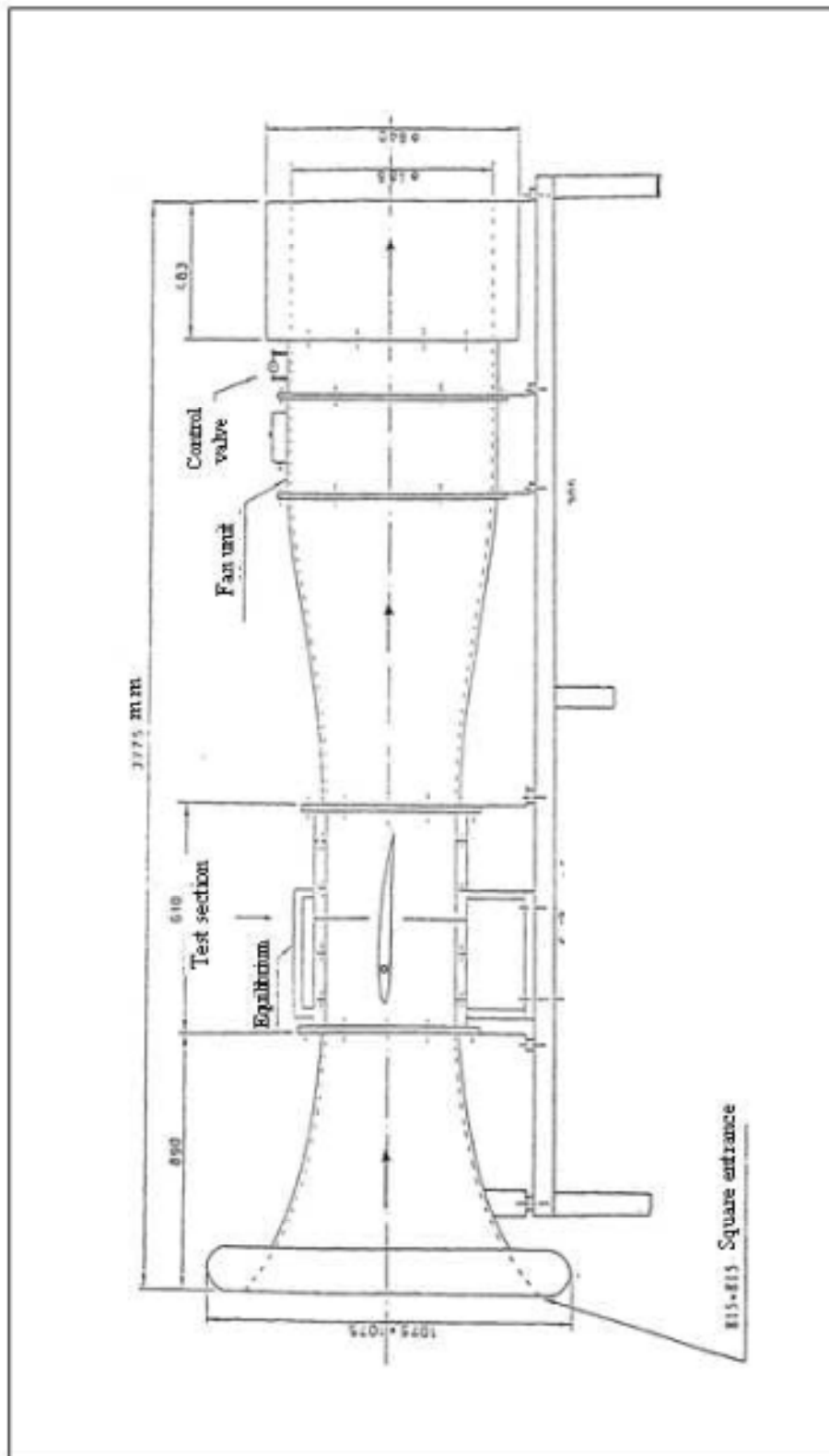


Fig.(1a) Subsonic wind tunnel

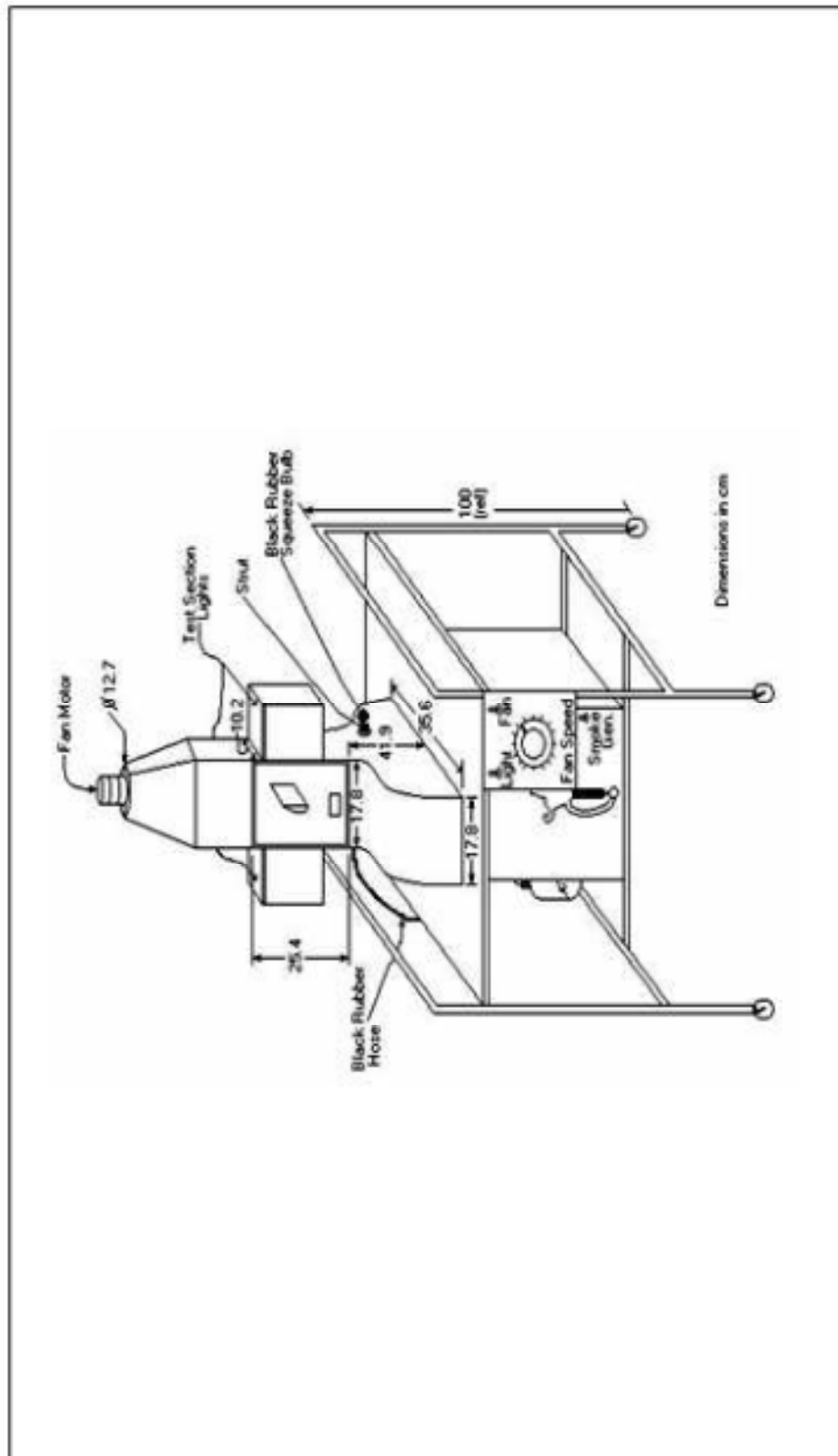
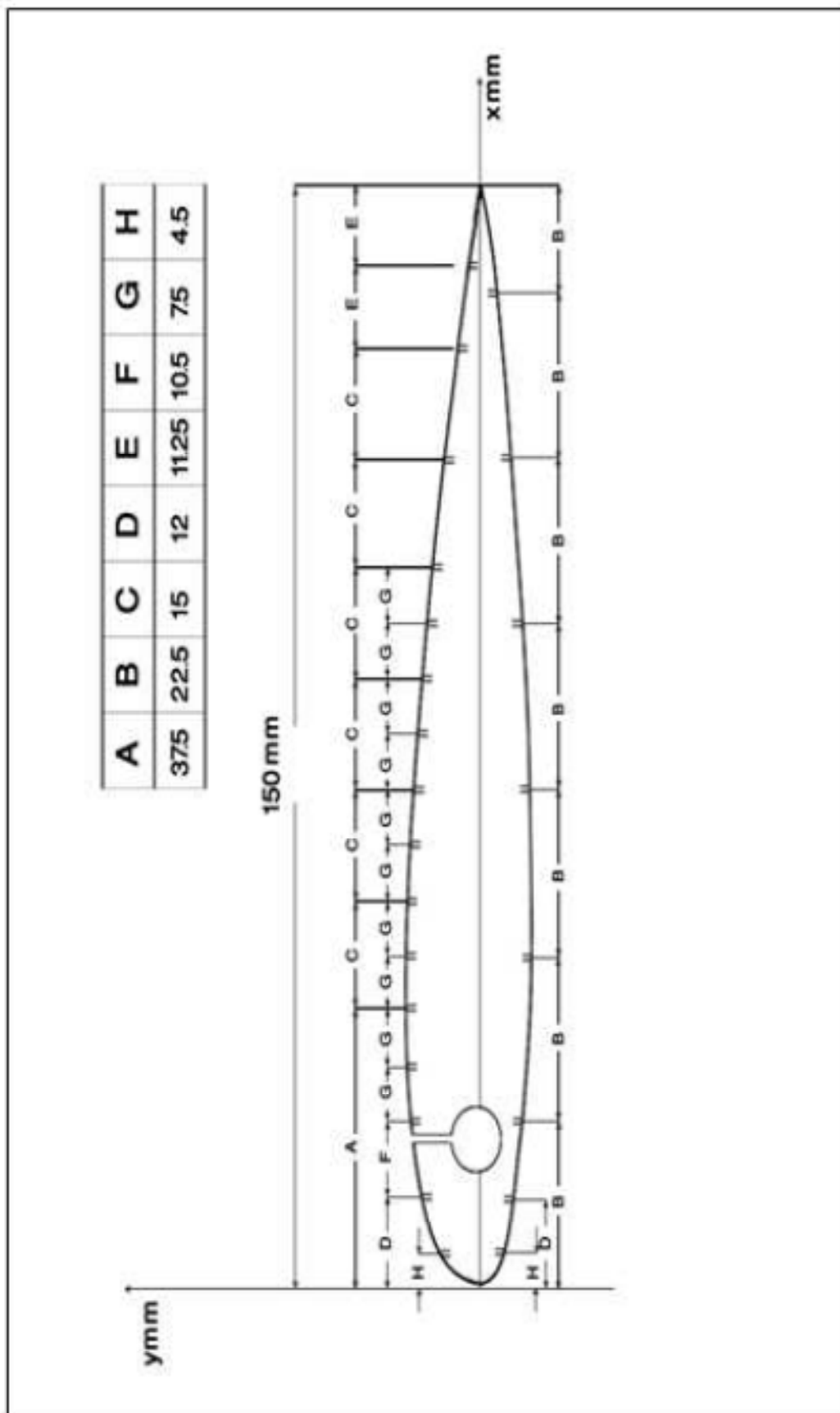


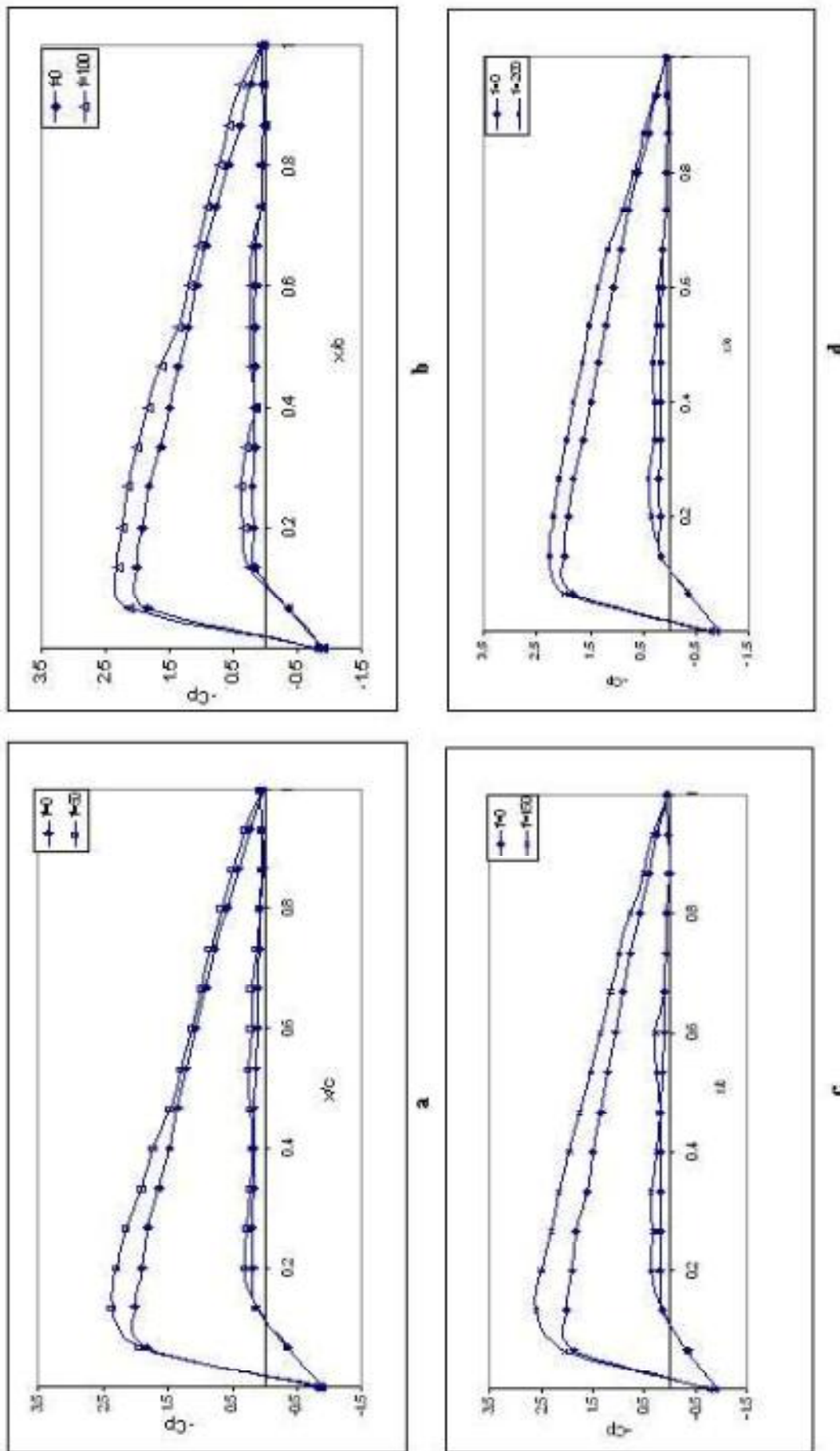
Fig.(1b) Smoke Wind Tunnel.



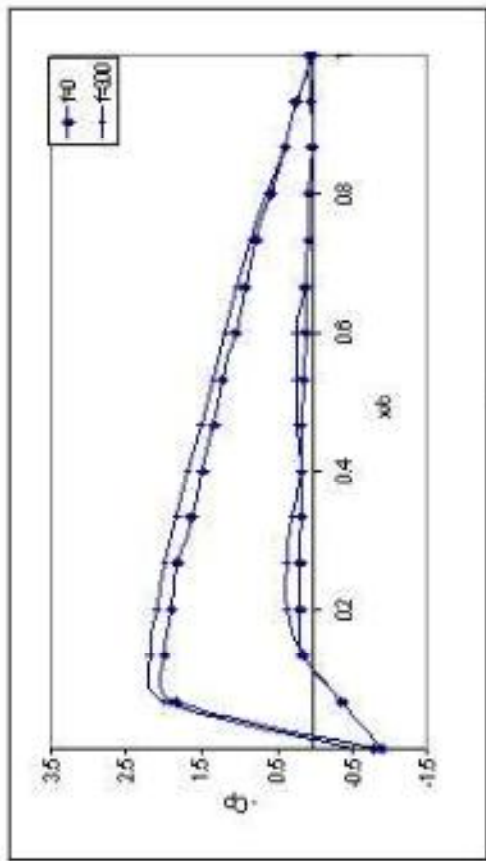
Fig.(1c) Model A,B,C, and D Airfoils.



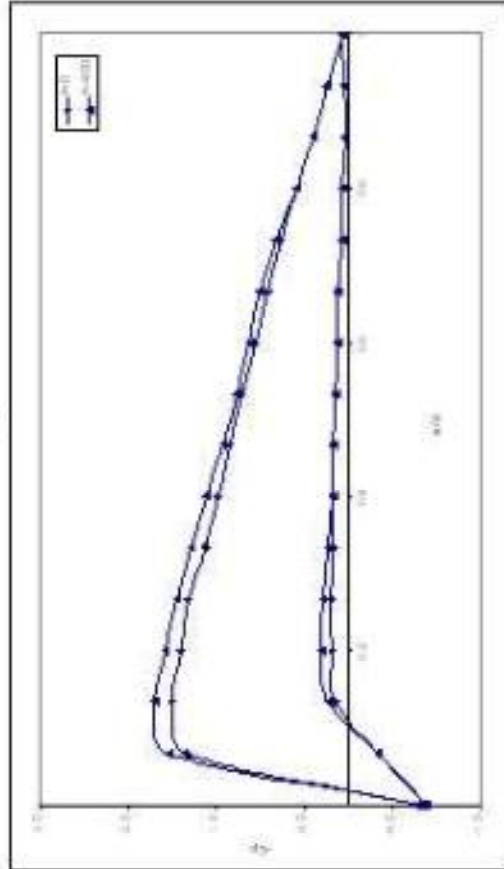
Fig(1d) Front view of airfoil section .



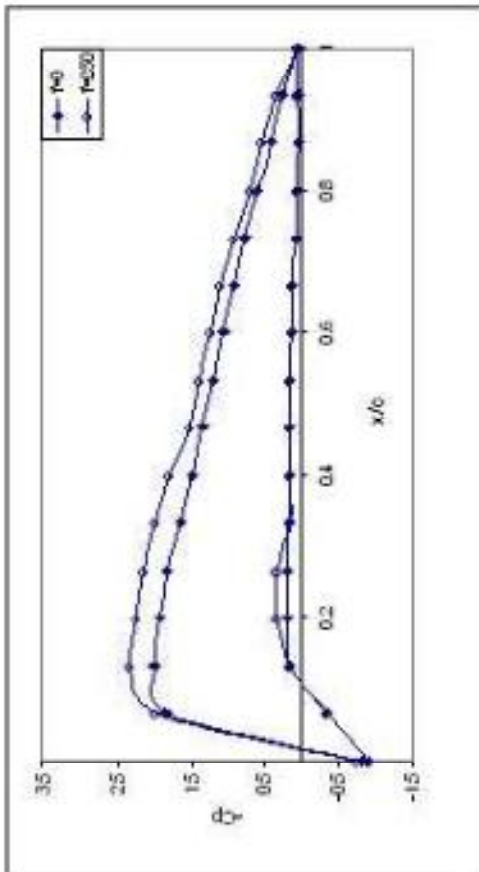
Fig(2) Presser distribution over an airfoil (NACA 23015) for a 9 deg angle of attack and excitation at 11.5% chord with frequency a) $f=50$ Hz, b) $f=100$ Hz, c) $f=150$ Hz, d) $f=200$ Hz, e) $f=250$ Hz, f) $f=300$ Hz, g) $f=350$ Hz, h) $f=400$ Hz



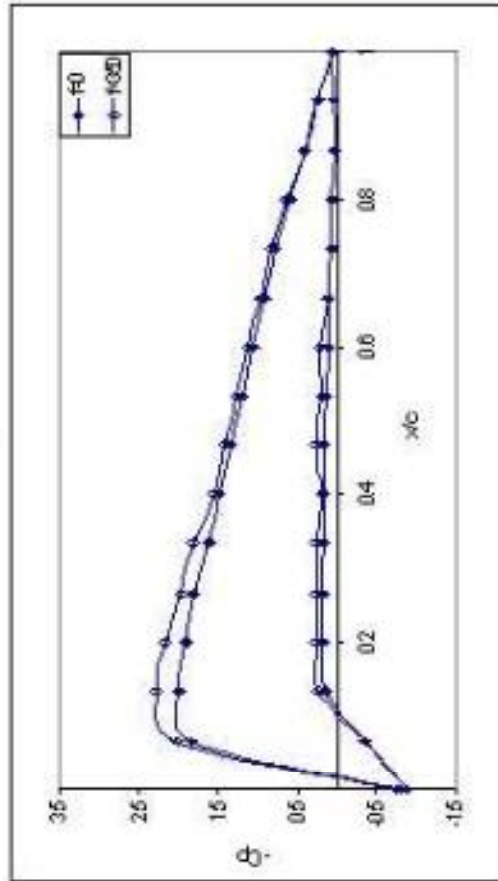
f



h

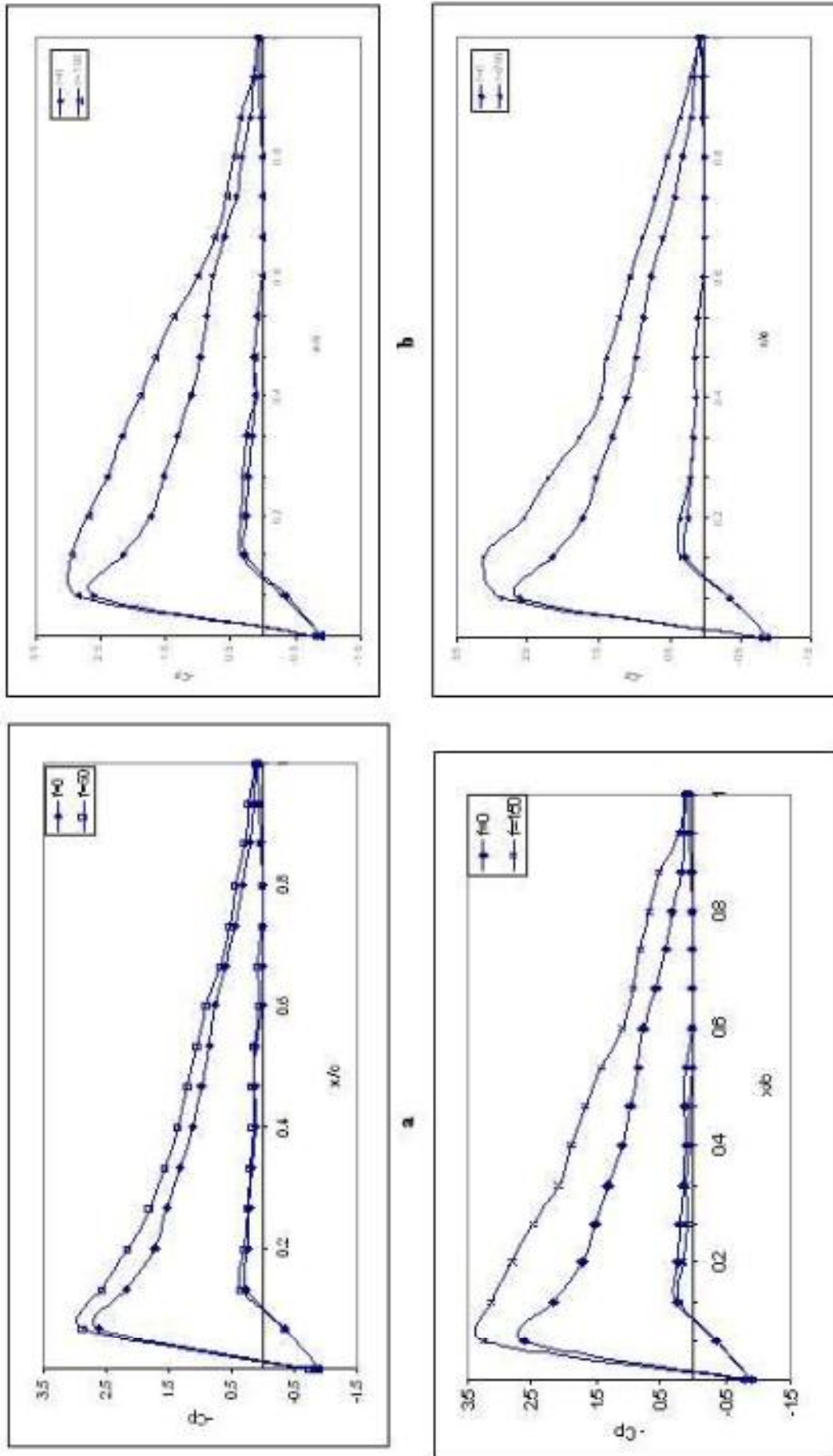


e

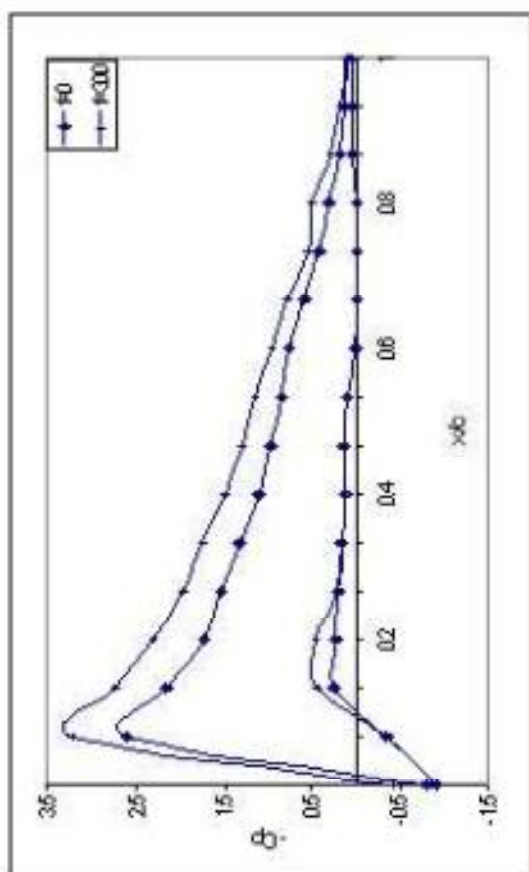


g

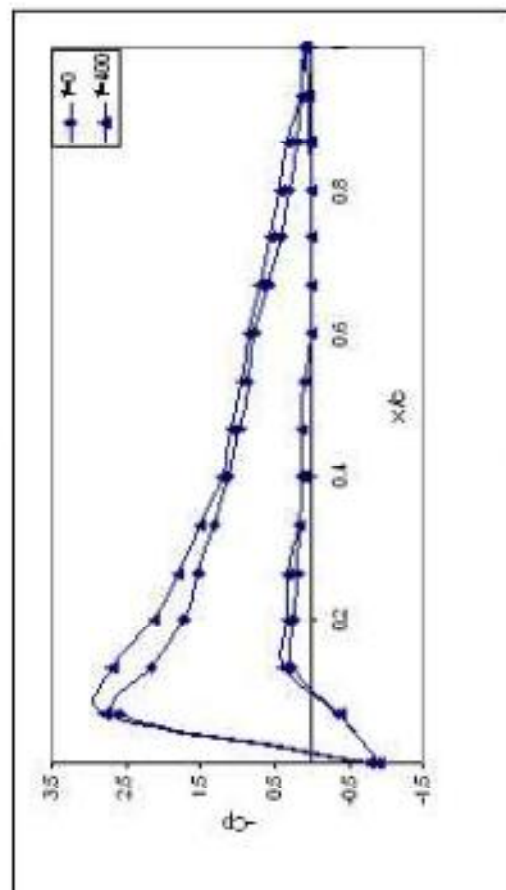
Fig. (2): Contd



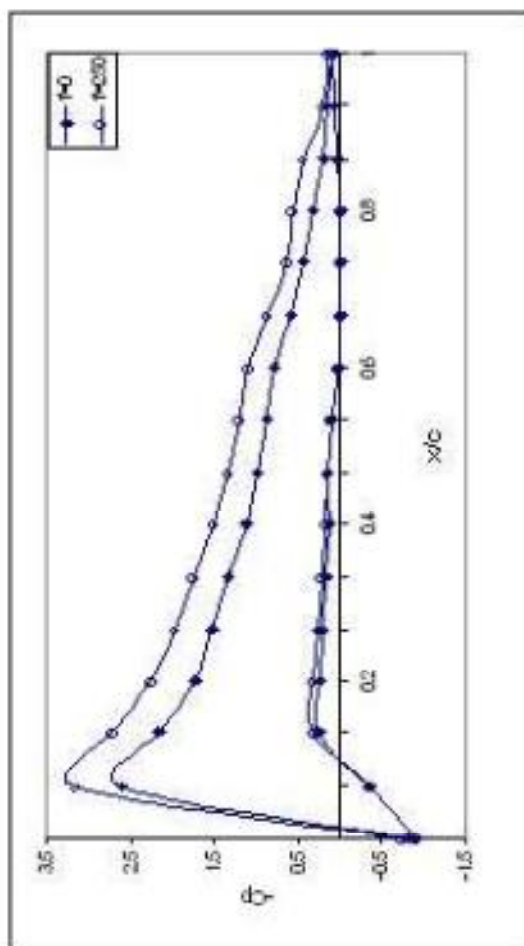
Fig(3) Presser distribution over an airfoil (NACA 23015) for a 12 deg. angle of attack and excitation at 11.5% chord with frequency a) $f=50$ Hz, b) $f=100$ Hz, c) $f=150$ Hz, d) $f=200$ Hz, e) $f=250$ Hz, f) $f=300$ Hz, g) $f=350$ Hz, h) $f=400$ Hz



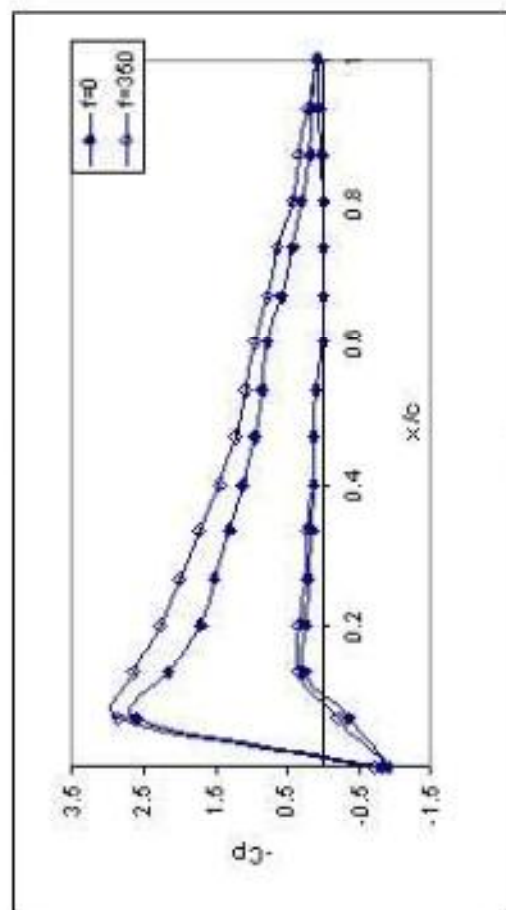
d



e



f



g

Fig. (3): Contd.

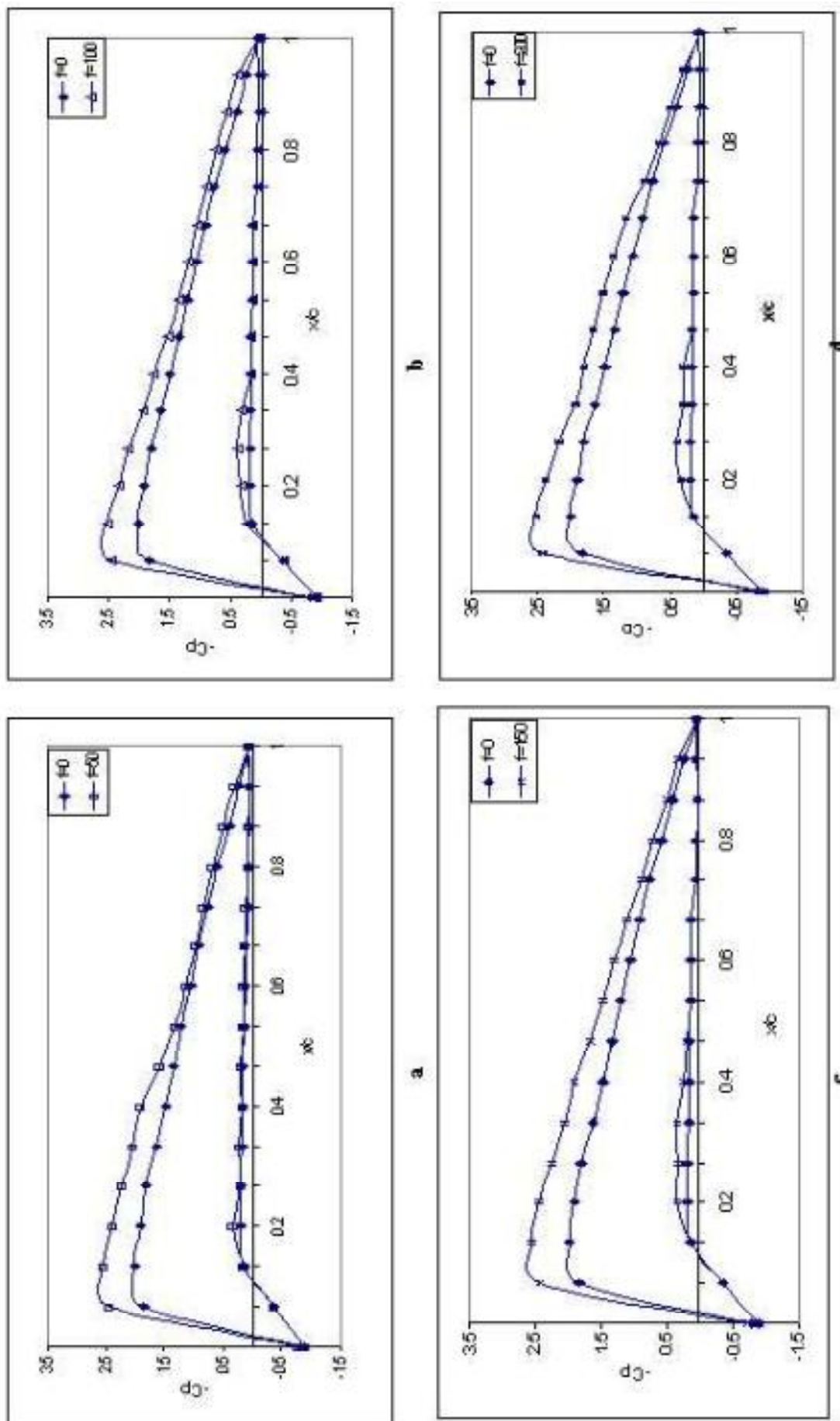


Fig.(4) Pressure distribution over an airfoil (NACA 23015) for a 9 deg. angle of attack and excitation at 6% chord with frequency a) $f=50$ Hz, b) $f=100$ Hz, c) $f=150$ Hz, d) $f=200$ Hz, e) $f=250$ Hz, f) $f=300$ Hz, g) $f=350$ Hz, h) $f=400$ Hz

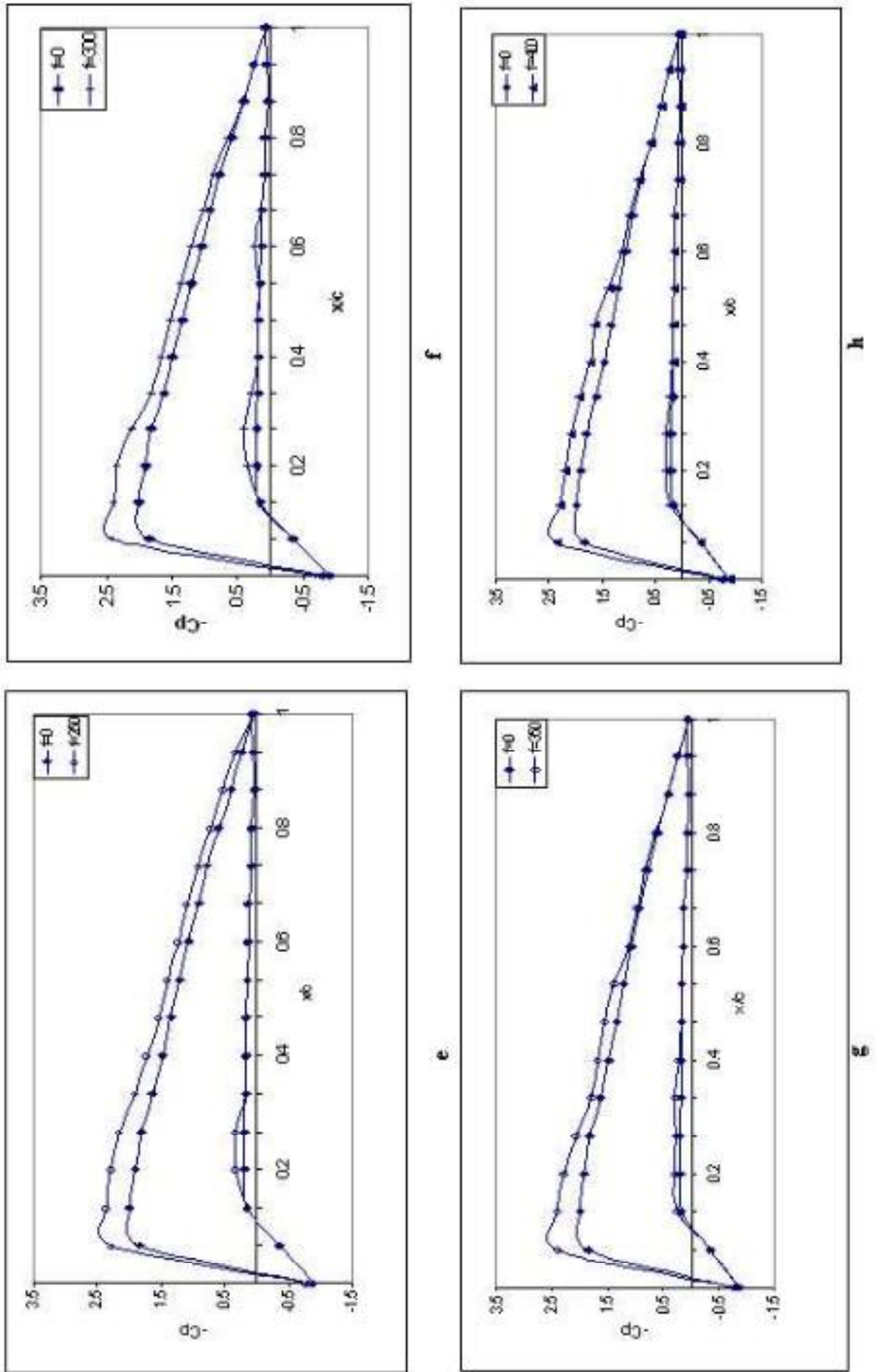
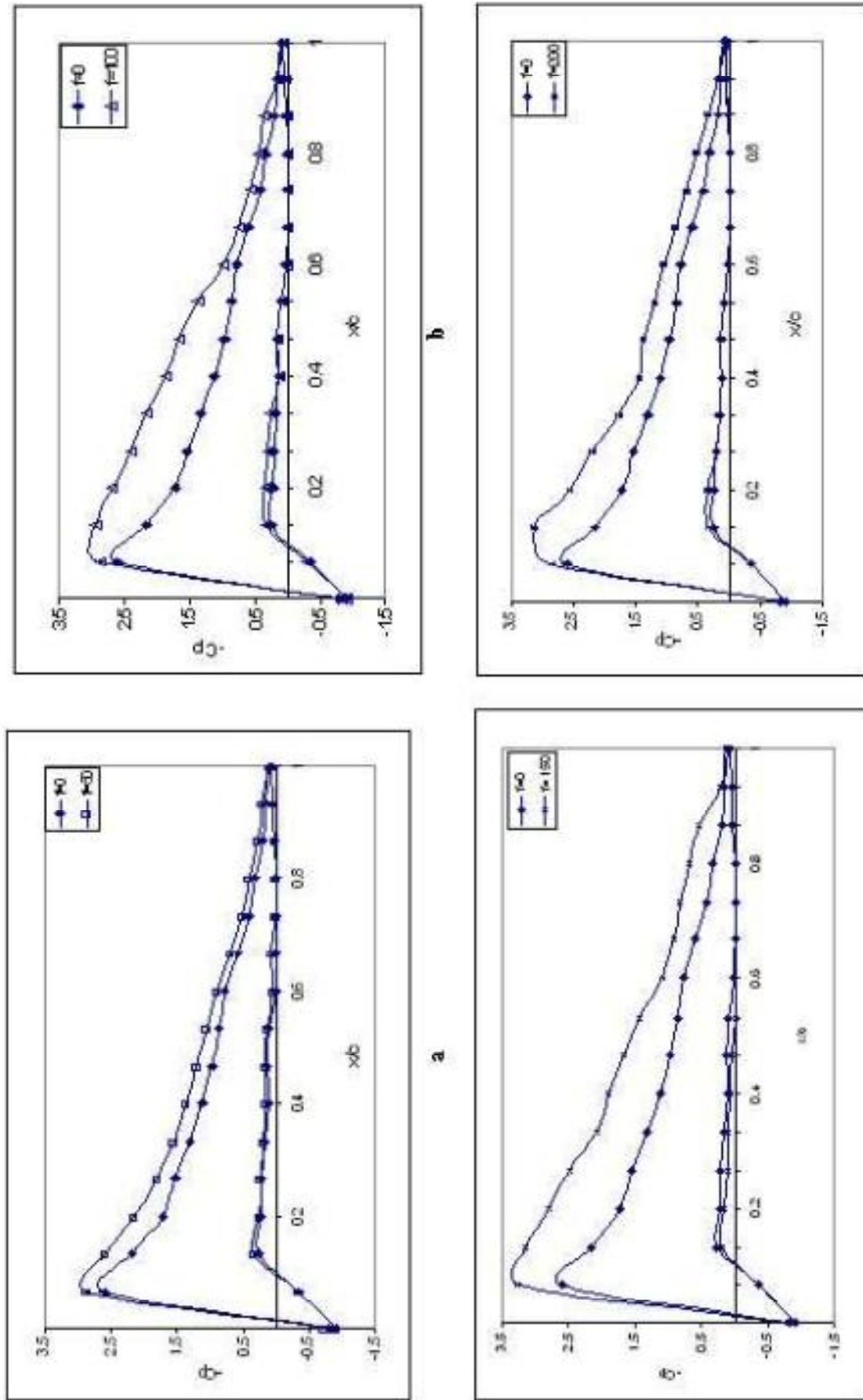
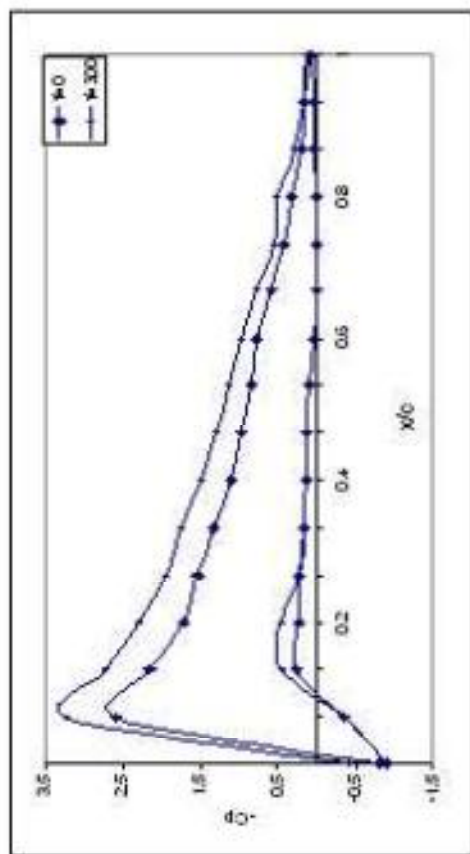


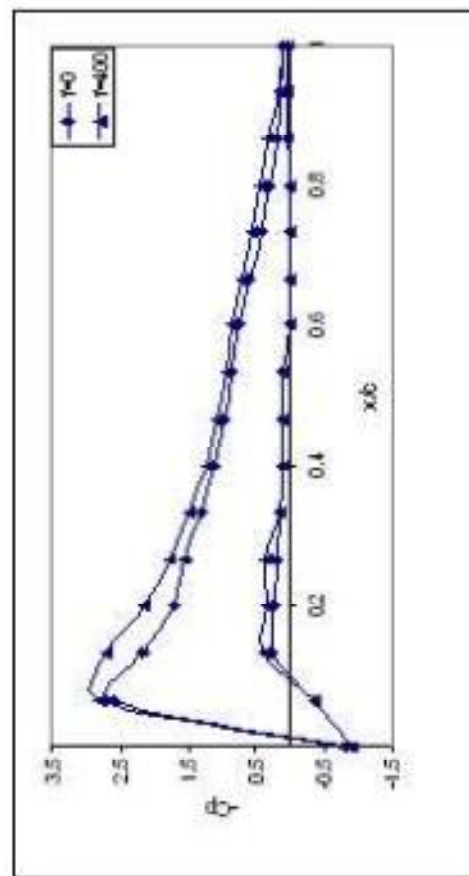
Fig (4): Contd



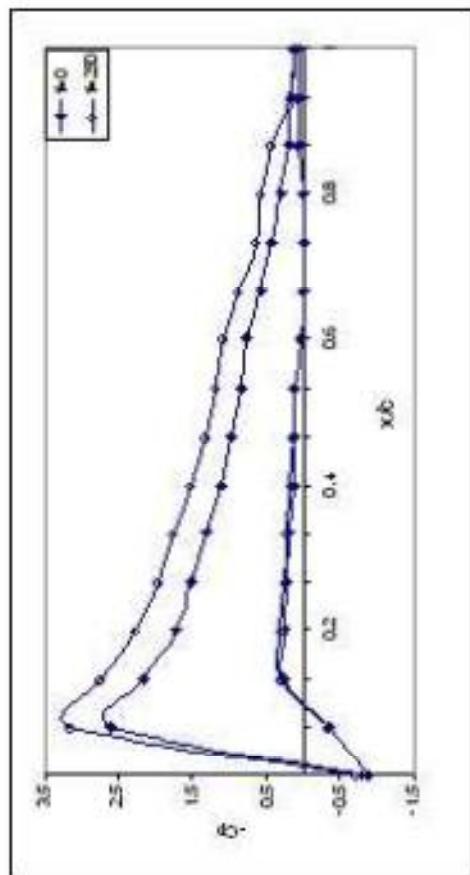
Fig(5) Presser distribution over an airfoil (NACA 23015) for a 12 deg. angle of attack and excitation at 6% chord with frequency a) $f=50$ Hz, b) $f=100$ Hz, c) $f=150$ Hz, d) $f=200$ Hz, e) $f=250$, f) $f=300$ Hz, g) $f=350$, h) $f=400$.



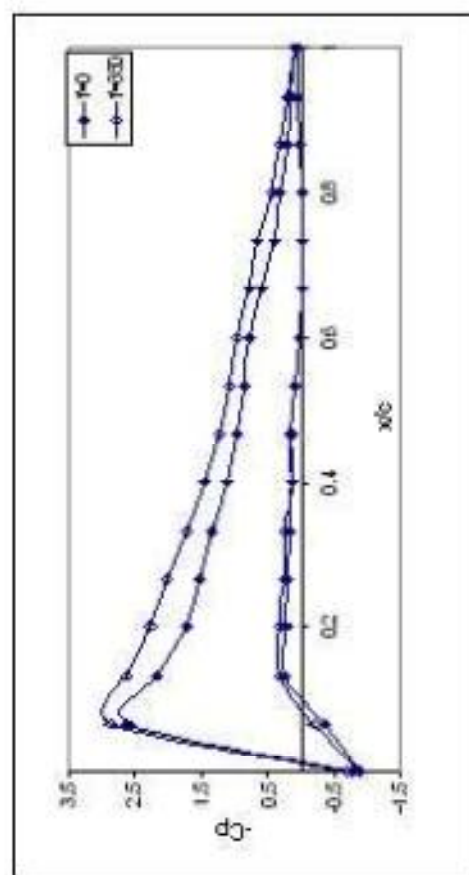
f



h



e



g

Fig. (5): Contd

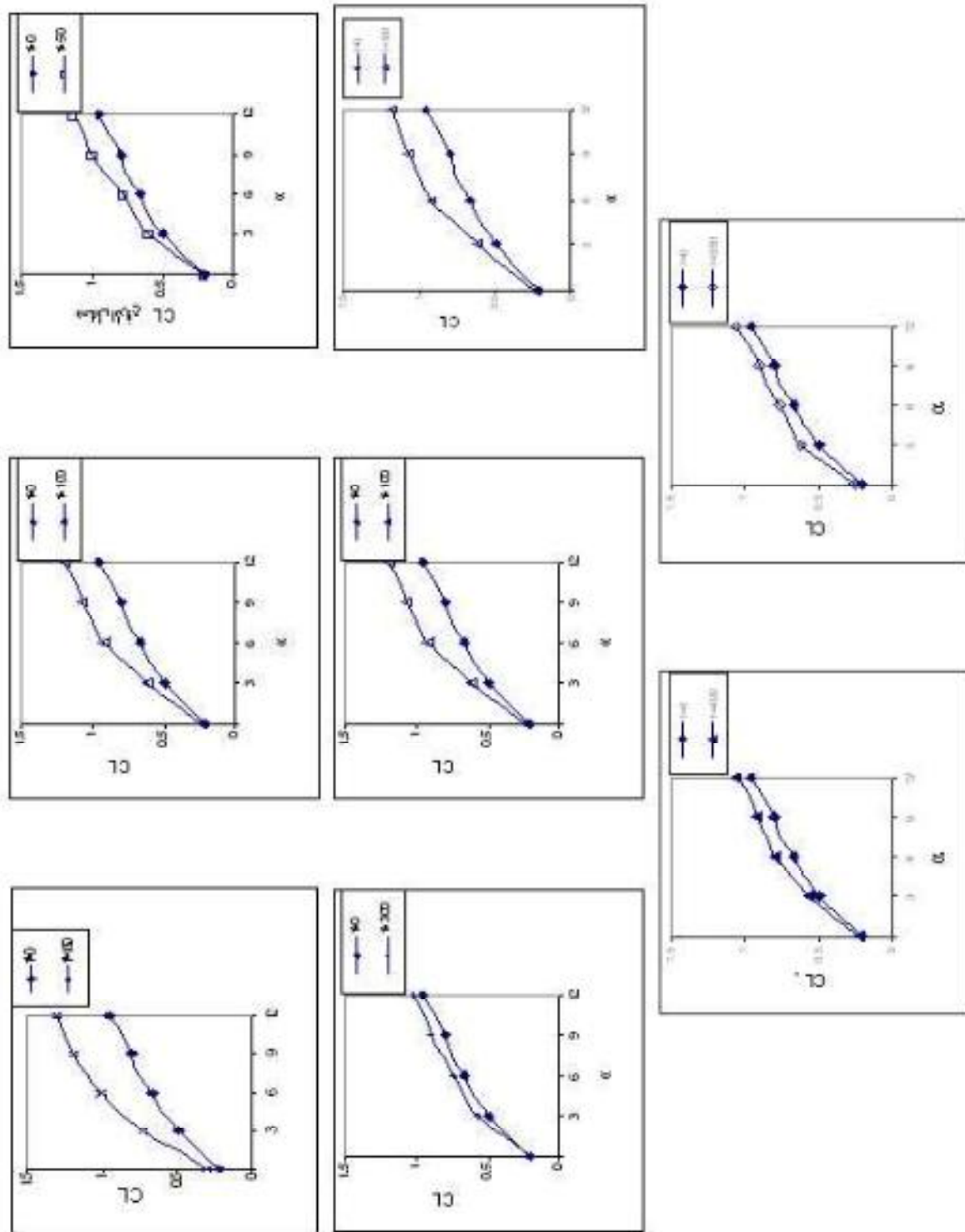


Fig.(6) Variation of lift coefficient(CL) over an airfoil (NACA 23015) at excitation 11.5% chord with angle of attack($\alpha=0-12$) deg. and different frequency value.

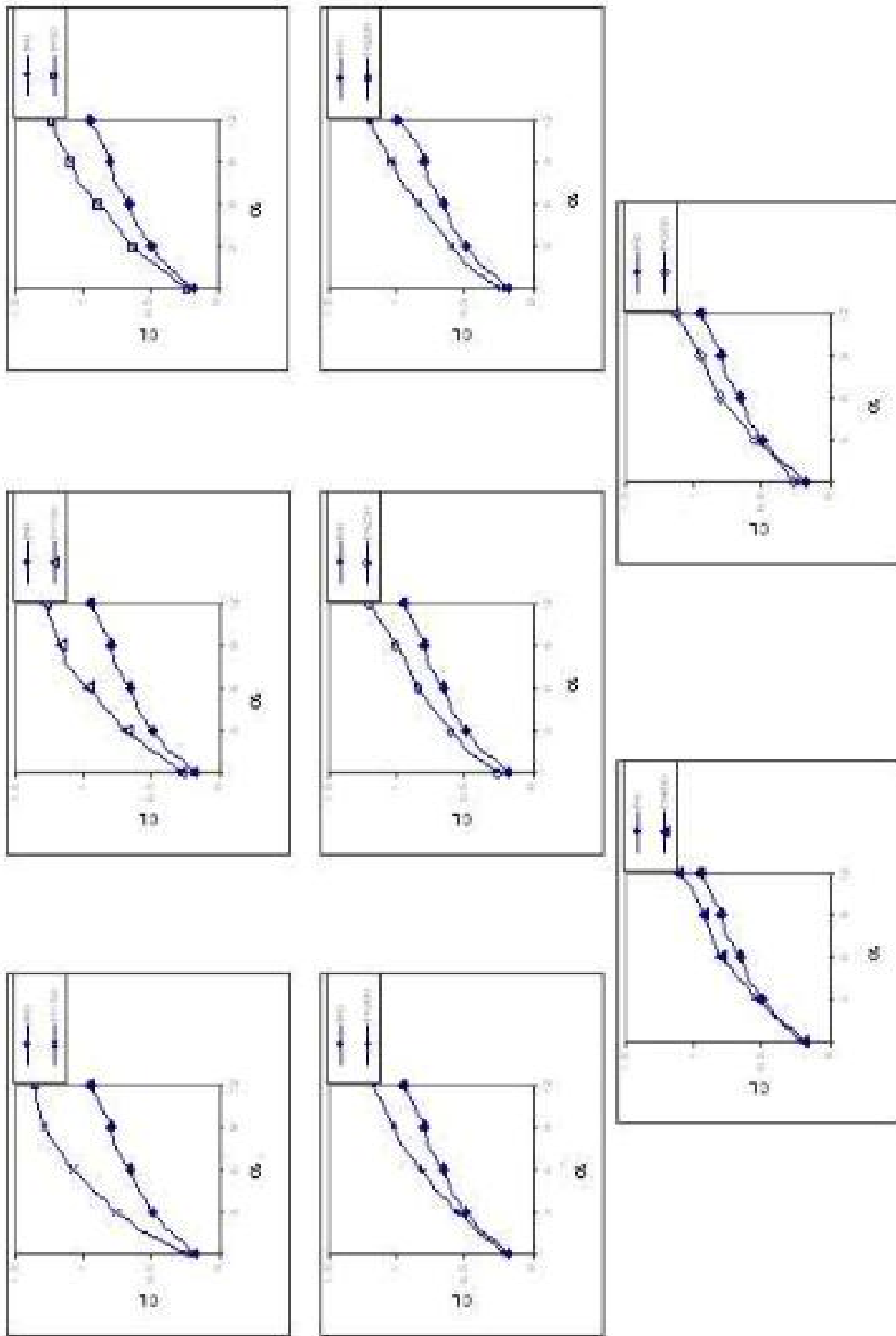


Fig.(7) Variation of lift coefficient(CL) over an airfoil (NACA 23015) at excitation 6% chord with angle of attack ($\alpha=0-12$) deg. and different frequency value.

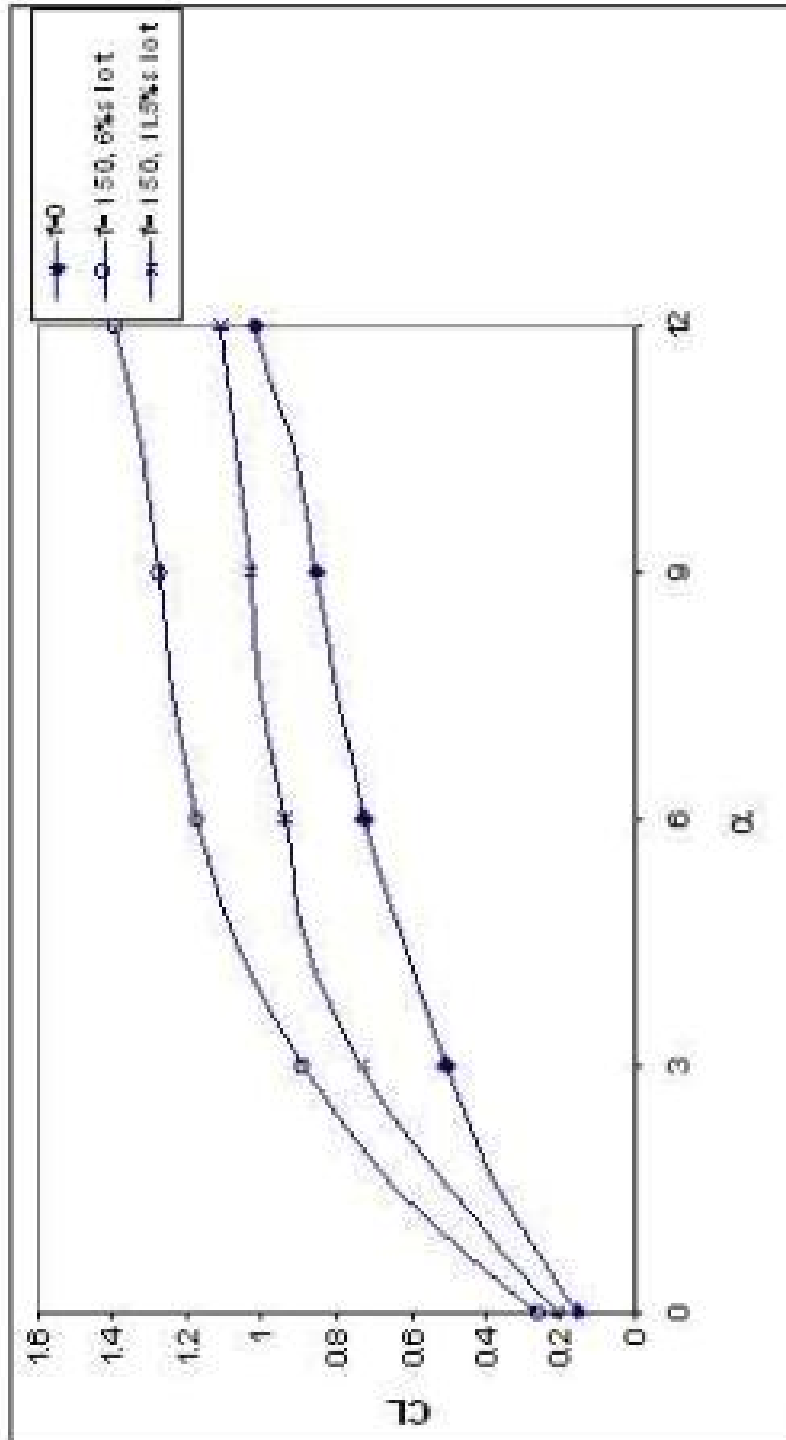
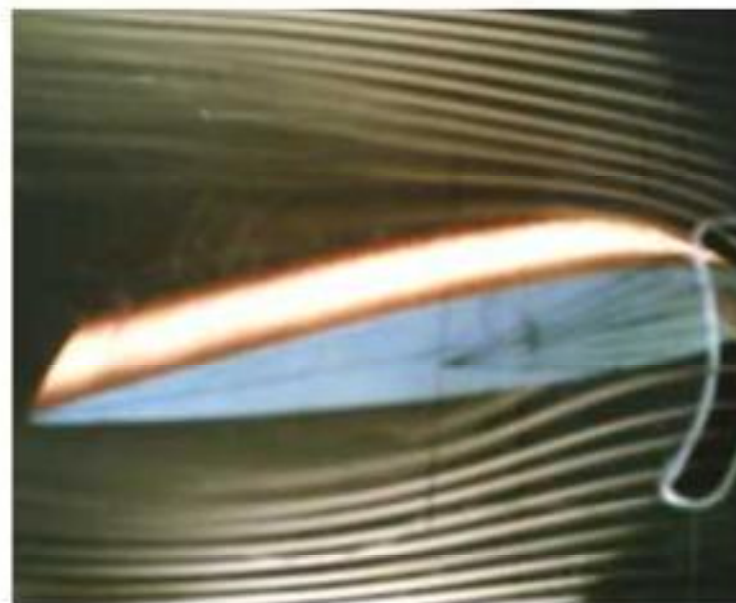


Fig (8) Comparison of lift coefficient curves over an airfoil (NACA23015) at excitation 6% & 11.5% chord with angle of attack :



1.50 Hz Excitation
At location 11.5 % chord



1.50 Hz Excitation
At location 6 % chord



No Excitation

Fig(9) Comparison of flow patterns over an airfoil for a 12 deg. angle of attack.

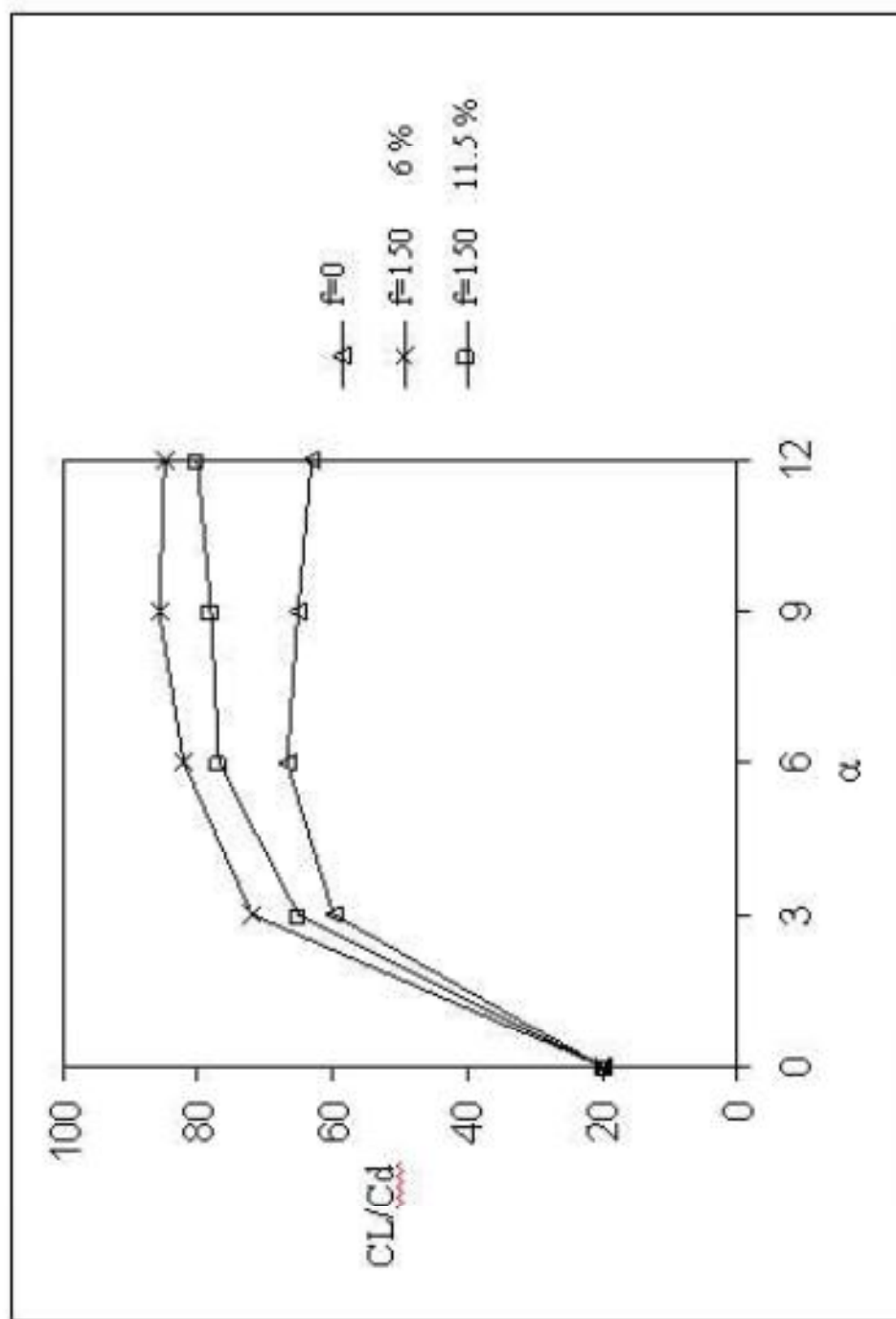


Fig.(10) Comparison of lift coefficient to drag coefficient (CL/C_d) curves over an airfoil (NACA23015) at excitation 6% & 11.5 % chord with angle of attack.

تأثير الإثارة الصوتية الداخلية على تحسين الخصائص الديناهووائية على الجنيح

د.اخلاص محمد فياض
قسم هندسة المكنان والمعدات
الجامعة التكنولوجية

الخلاصة:

درس تأثير الإثارة الصوتية الداخلية على الحافة الأمامية للجنيح ، انفصال الطبقة المتاخمة و أداء الديناهووائية لمقطع جناح (NACA23015) بدلالة موقع الإثارة لمدى من الترددات الصوتية (٤٠٠-٥٠). أجريت مجموعة من التجارب ، المجموعة الأولى أجريت في نفق هوائي مفتوح عند عدد رينولدز محسوب على أساس المتر (3.3x10⁵) لقياس توزيع الضغط لزوايا هجوم (0°، 3°، 6°، 9°، 12°). المجموعة الثانية أجريت في نفق الدخان لإظهار الجريان لزوايا هجوم (12°). أظهرت النتائج ان تردد و موقع الاثارة هما العاملان الاساسيان في تغير خصائص الجريان و تحسين خصائص الديناهووائية. ان أفضل تردد اثارة وجد بالقرب من تردد العتبة مع موقع إثارة قريب من نقطة الانفصال إضافة الى ذلك زيادة في الرفع و انخفاض في الكبح. كما لوحظ في إظهار الجريان ان الطبقة المتاخمة تعيد تلامسها مع السطح.